Magnetospheric Multiscale Mission Attitude Dynamics: Observations from Flight Data

Trevor Williams[1], Seth Shulman[2], Joseph Sedlak[3], Neil Ottenstein[4] and Brian Lounsbury[2]
NASA Goddard Space Flight Center, Greenbelt, MD 20771

The NASA Magnetospheric Multiscale mission, launched on Mar. 12, 2015, is flying four spinning spacecraft in highly elliptical orbits to study the magnetosphere of the Earth. Extensive attitude data is being collected, including spin rate, spin axis orientation, and nutation rate. The paper will discuss the various environmental disturbance torques that act on the spacecraft, and will describe the observed results of these torques. In addition, a slow decay in spin rate has been observed for all four spacecraft in the extended periods between maneuvers. It is shown that this despin is consistent with the effects of an additional disturbance mechanism, namely that produced by the Active Spacecraft Potential Control devices. Finally, attitude dynamics data is used to analyze a micrometeoroid/orbital debris impact event with MMS4 that occurred on Feb. 2, 2016.

I. Introduction

THE NASA Magnetospheric Multiscale (MMS) mission is flying four spinning spacecraft in highly elliptical orbits to study the magnetosphere of the Earth [1]. Launch on an Atlas V 421 occurred from Kennedy Space Center on Mar. 12, 2015, with insertion into a high-eccentricity orbit that was designed to satisfy a complicated set of science and engineering constraints [2]. After roughly 5 months of commissioning, the spacecraft have been flown in tetrahedron formations of varying dimensions in order to perform magnetospheric science measurements. In the first phase of the mission, these measurements are being taken on the dayside of the Earth, in a Region of Interest surrounding the apogee of the MMS orbit (radius 12 R_E). The goal during Phase 1 is to observe the magnetospheric reconnection events that are expected to occur near the bow shock where the solar wind impinges upon the magnetosphere. Measurements during the later Phase 2b, after apogee radius has been increased to 25 R_E, will be taken in the magnetotail [3], similarly to observe nightside magnetic reconnection events. Taking simultaneous measurements from four spacecraft allows spatial derivatives of the electric and magnetic fields to be determined, allowing variations that are functions of distance to be distinguished from those that are functions of time.

This paper describes the details of the attitude behavior that has been observed in MMS flight data. The MMS spacecraft spin at a nominal rate of 3.1 RPM, with spin axis nearly aligned with Ecliptic North, but tipped around 3 deg towards the Sun. Maintaining this tip towards the Sun requires that the spin axis be reoriented periodically (on the order of every month). Several booms are used to deploy instruments: two 5 m magnetometer booms in the spin plane, two rigid booms of length 12.5 m along the positive and negative spin axes, and four flexible wire booms of length 60 m in the spin plane. Reorientations of the spacecraft spin axis are kept to a minimum, so as to avoid exciting flexible motion of the wire booms. Slews are therefore generally limited to attitude maneuvers required to counteract the effects of gravity-gradient torques (which act mainly around the 1.2 R_E radius perigee of the highly eccentric MMS orbit) and apparent solar motion. As a consequence, orbital translational maneuvers (for formation flying) are carried out in the nominal science attitude. All attitude and delta-v maneuvers are executed using of a set of monopropellant hydrazine thrusters: two (of thrust 1 lbf) are directed along the spin axis in each direction, and eight (of thrust 4 lbf) in the spin plane; the latter are pulsed at the spin rate to produce a net delta-v. The on-board

[1] MMS Flight Dynamics Lead, Navigation and Mission Design Branch. Associate Fellow, AIAA. Phone: (443)545-4736.
[2] Aerospace Engineer, Honeywell Technology Solutions, Inc.
[3] Aerospace Engineer, ai Solutions, Inc.
[4] MMS Flight Dynamics Ground System Lead, ai Solutions, Inc.

controller [4] aims to null any attitude motion (e.g. nutation or spin axis shift) that is excited by delta-v maneuvers. These maneuvers are also then followed by attitude maneuvers to carry out any specified spin rate and spin axis orientation adjustments. The attitude maneuver controller also acts to damp down boom vibrations.

Extensive flight data is being collected throughout the mission that includes quantities that are of interest for attitude dynamics studies such as spin rate, spin axis orientation, nutation rate, etc. [5]. The paper will discuss the various environmental disturbance torques that act on the spacecraft, and will describe the observed results of these torques. In addition, a slow decay in spin rate has been observed to occur for all four spacecraft in the extended periods between maneuvers. It is shown that this despin is consistent with the effects of an additional disturbance mechanism, namely that produced by the Active Spacecraft Potential Control (ASPOC) devices: these emit positive indium ions to keep the MMS spacecraft electrically neutral, so as not to corrupt the electric field observations that are made by some of the on-board instruments. Finally, attitude dynamics data was key to analyzing an event in Feb. 2016 when the MMS4 spacecraft was struck by a small, high-speed object: this impact will be analyed in detail in the paper.

II. Environmental Torques

There are a number of conditions deriving from the operation of the science instruments that drive the MMS attitude requirements. In particular, the spin axis must be near the ecliptic pole to ensure that sunlight does not fall on the upper deck of the spacecraft. Illumination of the upper deck would cause the emission of photoelectrons, which would perturb the local plasma and affect the field measurements. However, the spin axis needs to be tilted by some angle from the ecliptic pole toward the Sun. This angle must be large enough to prevent shadows from the pre-amplifiers located 1.75 m from the tips of the long wire booms from crossing the spherical detectors at the ends of the booms. Any shadowing would cause a momentary interruption of the photo-emissive electron cloud around each sphere every spin period, which would again perturb the accuracy of the field measurements.

A compromise spin axis target box for science operations that satisfies the illumination conditions was chosen to be approximately an isosceles trapezoid on the sphere, having dimensions of roughly 2.5 deg × 2.5 deg and with a center offset from the ecliptic pole toward the Sun by approximately 3.5 deg. The MMS Attitude Ground System (AGS) must predict when the spin axis will drift to the edge of this box and then plan a slew to the opposite side of the box in order to maximize the time between attitude maneuvers. This is the "smart targeting" algorithm in the AGS, which accounts for the Sun and target box geometry and the seasonally changing environmental torques.

The dominant environmental torque driving attitude drift is caused by gravity-gradient forces. The torques from atmospheric drag and solar pressure are smaller by a few orders-of-magnitude. Very roughly, the order-of-magnitude of the gravity-gradient torque is 10^{-4} N-m, the solar pressure torque is less than 10^{-6} N-m, and the aerodynamic drag torque is less than 10^{-7} N-m. Only the gravity-gradient torque is considered in the environmental model for predicting the MMS spin angular momentum direction.

Ref. 6 gives the following expression for the spin-averaged and orbit-averaged gravity-gradient torque

$$\boldsymbol{\tau}_{gg} = \frac{3}{2}\frac{\mu}{a^3(1-e^2)^{3/2}}(I_z - I_t)\left(\hat{\boldsymbol{Z}}\cdot\hat{\boldsymbol{h}}\right)\left(\hat{\boldsymbol{Z}}\times\hat{\boldsymbol{h}}\right), \tag{1}$$

(with corrected factor of 1/2). The factor μ is the Earth's gravitational constant, a is the MMS semimajor axis, e is the eccentricity, I_z is the major principal moment of inertia, I_t is the transverse moment of inertia (taken as the mean of the x- and y-inertias), $\boldsymbol{Z}$ is the direction of the body spin axis, $\boldsymbol{h}$ is the vector normal to the orbit plane, and the carets indicate unit vectors. The inertia tensor here is computed as though the booms were rigid since the characteristic time scale for the gravity-gradient perturbations is much longer than the period of the vibrational modes of the wire booms. This is in distinction from the effective inertia tensor used in the onboard attitude control system that accounts in part for the flexibility of the spacecraft.

Application of Eq. (1) to the MMS angular momentum vector yields predictions for the spin axis precession. In [5], these predictions have been compared to the observed drift of the spin axis at various stages early in the MMS mission. Table 1 shows a sample of these results for MMS1 (results for the other three probes are similar). The first row shows results for the precession after deployment of the magnetometer booms, but prior to deployment of the long, thin-wire, spin-plane double-probe (SDP) booms. The second row shows results for times during the multi-step SDP deployment, and the last row shows results after SDP deployment was complete.

Table 1. MMS1 predicted and observed angular momentum precession averaged over several days.

Deployment Status	Predicted Precession per Day (deg)	Observed Precession per Day (deg)
Pre-SDP Deployment	0.0856	0.1052
During SDP Deployment	0.0565	0.1200
Post-SDP Deployment	0.0514	0.0513

Table 1 shows that the predictions of the angular momentum precession improved when the SDP was fully deployed. This improvement is attributed to a more accurate knowledge of the actual inertia tensor for the deployed configuration; the AGS uses a simple point mass model for the spooled SDP wire before and during deployment.

Fig. 1 presents the accumulated errors in the predicted precession angles for MMS2 after all booms were deployed (results are similar for the other three observatories). This plot shows a long time span when no maneuvers were performed. The prediction error is approximately 0.01 deg after one month of drift. These errors are smaller than the prelaunch error estimates by an order of magnitude due to better than anticipated knowledge of the inertia tensor values.

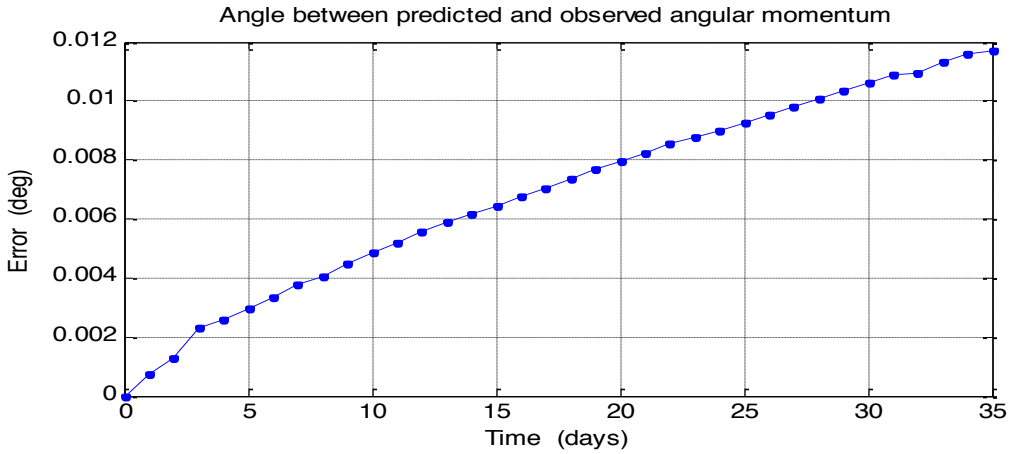

Figure 1. Angle between predicted and observed angular momentum vectors for MMS2.

There also is a seasonal variation in the gravity-gradient precession of the spin axis. There are several moving parts to this motion. First, due to the large semimajor axis, the MMS orbit normal vector drifts only slowly due to torque from the Earth's equatorial bulge. Nonetheless, over one year, the orbit normal has moved roughly 21 deg. Next, from the perspective of the MMS orbit, the Sun moves approximately one degree per day, and the center of the science target box moves around the ecliptic pole to follow it. Finally, the spin axis precession occurs within the target box and a maneuver is performed whenever it drifts to one edge of the box.

Due to the changing spin axis and orbit normal relative directions, the magnitude and direction of the precession computed from Eq. (1) also change. Fig. 2 shows the magnitude of the spin precession over the course of nearly one year. The discontinuities occur at the attitude maneuvers. These values should be compared to the target box motion of approximately 0.06 deg per orbit (this is the one degree per day motion of the Sun projected onto the unit sphere at the box center, 3.5 deg from the ecliptic pole). Unfortunately, when the precession magnitude is comparable to the motion of the target box, they are in opposite directions, implying a need for more frequent maneuvers. This angle is shown in Fig. 3, which presents the angle between the direction of motion of the center of the target box and the spin axis precession direction. This angle is large for most of the mission. The two motions are parallel only near the end of 2015. At that time, the maneuver frequency required for attitude maintenance was the smallest. The average time between maneuvers for the months around day 360 was 30 days, whereas the average time between maneuvers over the entire post-commissioning part of the mission has been 22.5 days. Of course, the maneuver frequency is driven by orbit and formation maintenance considerations (see [7] for further details) as well as attitude maintenance. The maneuver planning is carried out with both orbit and attitude in mind to keep the number of burns to a minimum.

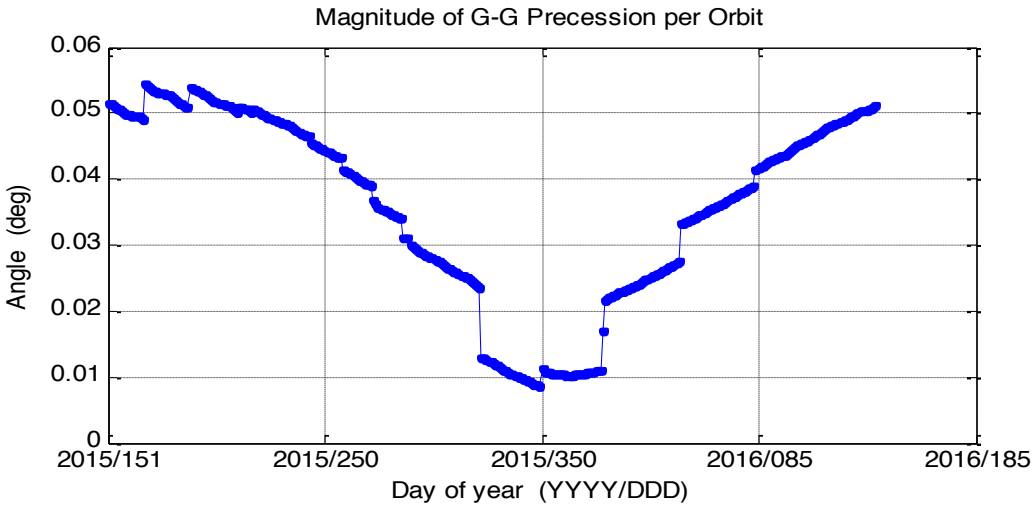

Figure 2. Magnitude of gravity-gradient driven spin axis precession per orbit.

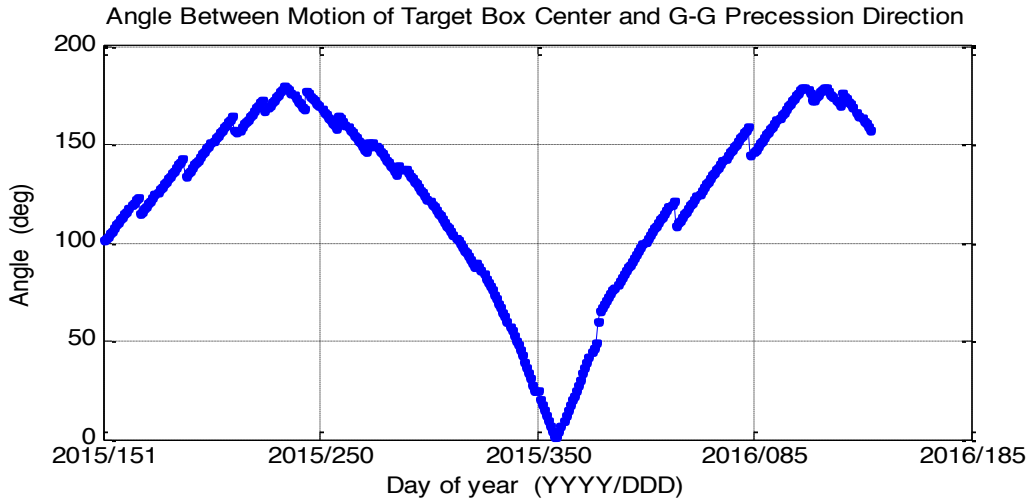

Figure 3. Angle between motion of target box center and direction of gravity-gradient driven spin axis precession.

III. Instrument-Related Torques

The MMS spacecraft interact with the plasma environment and build up a positive floating potential. The effects of this are degraded science measurements as well as decreased life of certain on board electronics. The Active Spacecraft Potential Control (ASPOC) instrument attempts to neutralize this relative potential by expelling positive indium ions. These instruments are also classified as Indium Field Emission Electric Propulsion (In-FEEP) thrusters by their manufacturer. Refs. 8 & 9 describes the research and development of these as potential micro-propulsion thrusters on future missions.

There are 2 ASPOC units per spacecraft, each with 4 indium ion emitters. Of these 8 total emitters per spacecraft, only 2 (one per unit) are active at a time. The emitter consists of an indium reservoir with a jet. There is an extractor electrode above the jet as seen in Fig. 4. A strong potential is created between the emitter and extractor. Once a strong enough electric field is formed, the indium atoms are ionized at the jet tip and accelerated by the same field as described in Ref. 8. This induces a thrust, on the order of micro-Newtons.

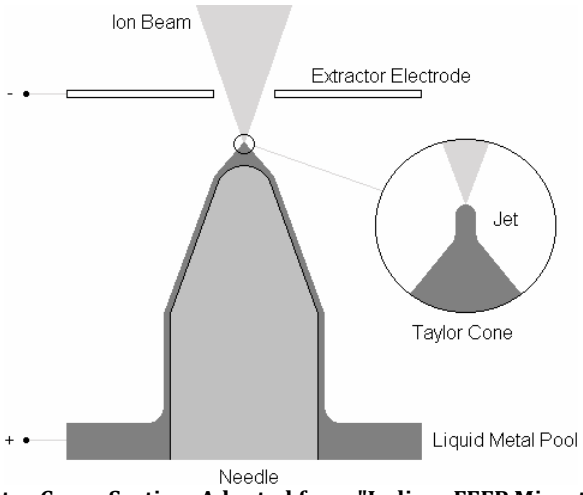

Figure 4. ASPOC Emitter Cross-Section. Adapted from "Indium FEEP Microthruster Experimental Characterization," by Tajmar, M., A. Genovese, and W. Steiger.

The emitters are oriented in such a way that they create a coupled, negative torque on the spacecraft z-axis. Negative is defined as against the nominal spin direction of the spacecraft. Each ASPOC is located in the same geometric location across the 4 observatories. However, four factors can change the effect these emitters have on each spacecraft: the spacecraft center of mass location (CM), the spacecraft moment of inertia (MOI), the active emitter pair, and the emitting energy across the four observatories.

The decay in the spacecraft spin rate for MMS1 can be seen in Fig. 5 (similar behavior is seen for the other observatories). The spikes are caused by a temporary spin rate increase when in shadow due to thermal contraction. The discontinuities are propulsive maneuvers. The emitters impart no measurable delta-V or precession, only a spin rate deceleration.

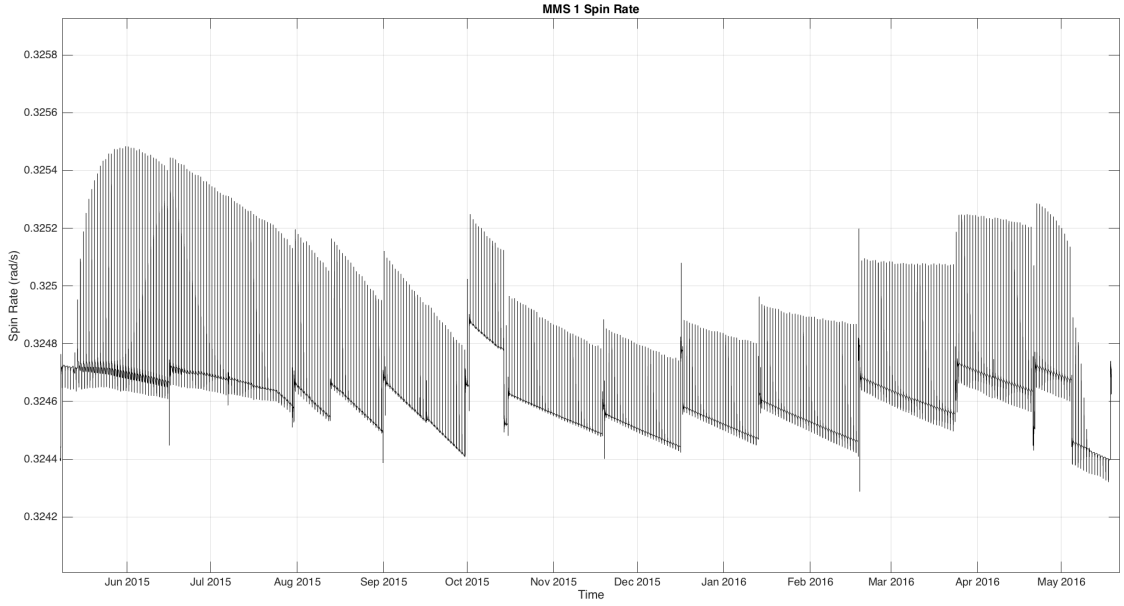

Figure 5. MMS 1 Spin Rate Post-Commissioning.

There are noticeable differences in the deceleration rate between the four spacecraft. This can be partially attributed to the four factors described above. The analysis performed took into account the CM location and MOI at

the time of the sample. The active emitter pair as well as their energies has been constant since the commissioning phase for each observatory.

There is spin rate decay present even before the ASPOC instrument was first activated on July 24, 2015. There are known phenomena (eddy currents, residual dipole interaction, etc) that can cause variation in spin rate. Since spinrate data is available prior to ASPOC activation, these effects can be biased out. The slight spinrate decay observed prior to July 24, 2015 was subtracted from the calculated deceleration for the time period that ASPOC is powered. Fig. 6 provides a zoomed in view with annotations for ASPOC power on and duty cycle change. There is a clear change in spinrate decay cooresponding to these times. These ASPOC activities were the only changes to the spacecraft at the time of the spinrate change, concluding that the ASPOC was responsible for the change in spinrate decay.

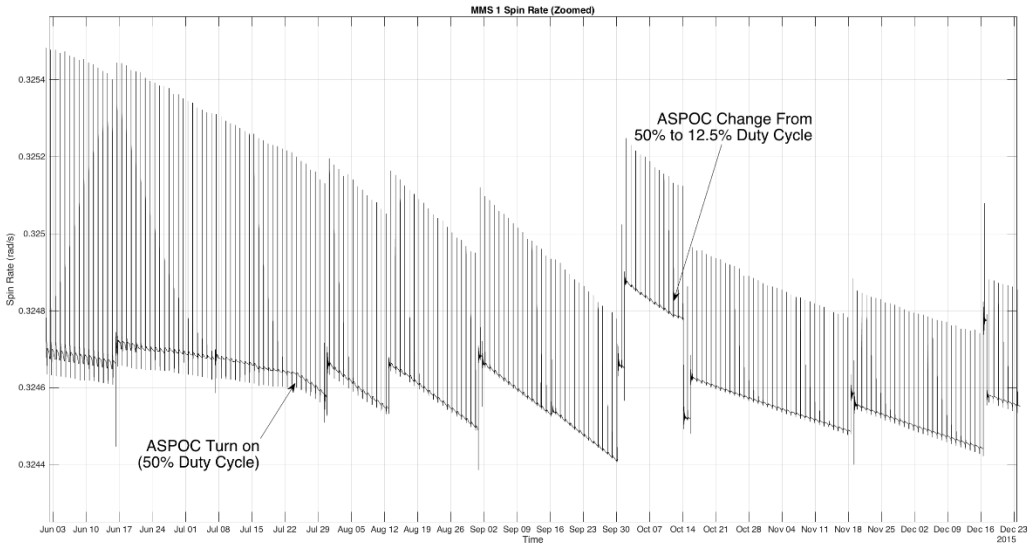

Figure 6. Zoom in on MMS 1 Spin Rate Post-Commissioning.

Using the geometry with respect to the CM and emitter location, the MOI at the sample time, and the deceleration, a thrust can be calculated for each sample. A sample is defined by the period between propulsive maneuvers where the deceleration was calculated. The deceleration value has been biased in order to account for spin rate decay due to known phenomena as explained above. These calculations were done at 13 sample intervals for each observatory. The resultant thrust value is an average between the two emitters, as individual thrust values cannot be derived since the emitters are always operated in pairs. The calculated thrust values from 13 samples across four observatories can be seen in Fig. 7.

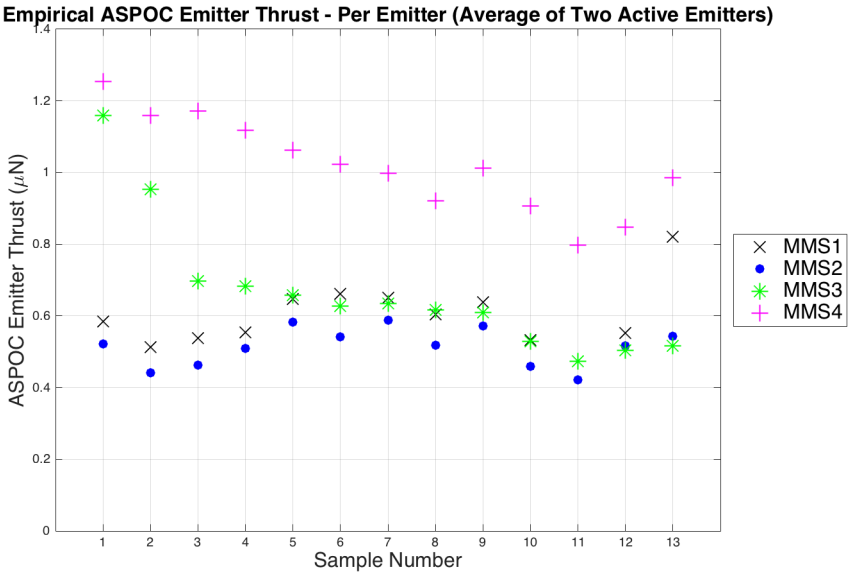

Figure 7. Calculated Thrust Imparted By ASPOC Emitters

Samples 1-4 correspond to a 50% duty cycle (12 hours per orbit) and samples 5-13 correspond to a 12.5% duty cycle (3 hours per orbit). The start of nominal ASPOC operations was officially stated to be Day of Year 244 in 2015: this corresponds to sample 3 and above. Although samples 1 and 2 yield data in the expected range, these should carry less weight. This is the suspected cause of the large apparent change in the observatory 3 thrust.

The acceleration of the relatively heavy indium ion results in a force on the order of micro-Newtons. Ref. 9 gives the following expression for the force generated by an emitter:

$$F = \dot{m_{ion}} v = (I_E - I_{Extr} - I_{PS}) \sqrt{\frac{2 m_{ion} V_E}{e}}\, c(I_E) \qquad (2)$$
$$= (I_B) \sqrt{\frac{2 m_{ion} V_E}{e}}\, c(I_E)\,,$$

where I_E is the emitter current, I_{Extr} is the extractor current, I_{PS} is the plume shield current, I_B is the beam current, m_{ion} is the indium ion mass, V_E is the emitter voltage, and $c(I_E)$ is the thrust coefficient factor. The thrust coefficient factor accounts for losses due to beam divergence. The thrust coefficient factor can typically can range between 70%-95% as shown from direct laboratory measurements by the manufacturer, and described in [9].

Table 2. Beam and Emitter Characteristics

Obs	Beam Current (I_B)	Emitter Voltage (V_E)
1	9.88E-06	5983
2	9.89E-06	6001
3	9.98E-06	6001
4	1.00E-05	6200

Using Eq. (2) and the beam/emitter characteristics in Table 2, the thrust coefficient factor can be calculated for each spacecraft. The beam/emitter characteristics were taken directly from spacecraft telemetry and averaged for each active emitter pair. The thrust coefficient factor will be an average between the two active emitters on each spacecraft, as it cannot be discerned if one emitter is providing more thrust than another. As the relation between

thrust and thrust coefficient factor is linear, Fig. 8 follows the same trend as Fig. 7.

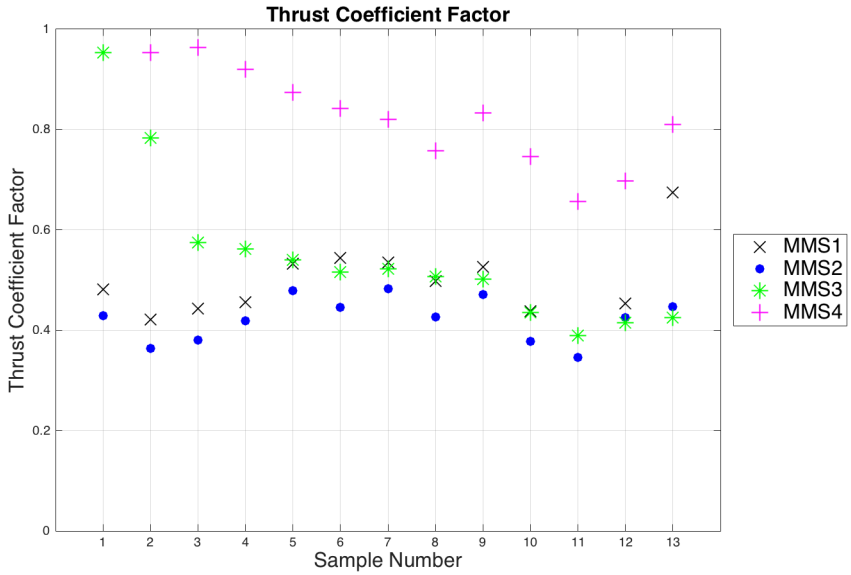

Figure 8. Calculated Thrust Coefficient Factor

The thrust coefficient factors for observatories 1-3 are lower than the expected values from the manufacturer. The reason for this is not entirely clear, and can be a focus of further research. Inquiries have been made in order to get more specifics on which variables can have slight effects on the thrust output of the emitters. However, there are numerous differences between the manufacterer's testing and on-orbit calculations. The tests were performed in a controlled laboratory environment, with different beam energies, emitter voltages, and thruster geometry than currently in use on MMS.

IV. Micrometeoroid/Orbital Debris Impact on MMS4

Attitude dynamics flight data was key to analyzing a suspected micrometeoroid/orbital debris (MMOD) strike on the MMS4 spacecraft that occurred on Feb. 2, 2016. This event, and the approach that was taken to analyzing it, will now be discussed.

A. Background

The MMS spacecraft each has five shunt circuits that are used to route excess electrical power that may be generated by the solar arrays. This excess power is then dissipated to space through four radiator panels (see Fig. 9-*left*), covered with fragile Optical Solar Reflector (OSR) material and located on the bottom (-Z) face of the spacecraft (see Fig. 9-*right*). Each of the five shunt circuits contains four 180 Ω resistors in parallel, one mounted behind each of the four radiator panels. On Feb. 2, 2016, it was observed that one of the MMS4 shunt circuits exhibited a drop of 25% in its maximum current (Fig. 10): this is consistent with losing the functionality of one of the 180 Ω resistors. Failure of this type of resistor due to workmanship issues is quite unlikely; furthermore, it was then determined that other spacecraft data exhibited suggestive signatures at the same time that the shunt resistor failed. In particular, in this same period the accelerometer data contained transients, small changes in both nutation angle and spin axis orientation were observed, and the star cameras showed spikes (Fig. 12-*red*) in the number of bright, non-star objects in the fields of view of the three operating Camera Head Units (CHUs). It should be noted that these cameras are located on the –Z face of the spacecraft, oriented in roughly the same direction as the radiator panels. The star camera system eventually autonomously rebooted itself after persistently failing to converge to an attitude determination solution (Fig. 12-*blue*) as a result of these multiple bright objects.

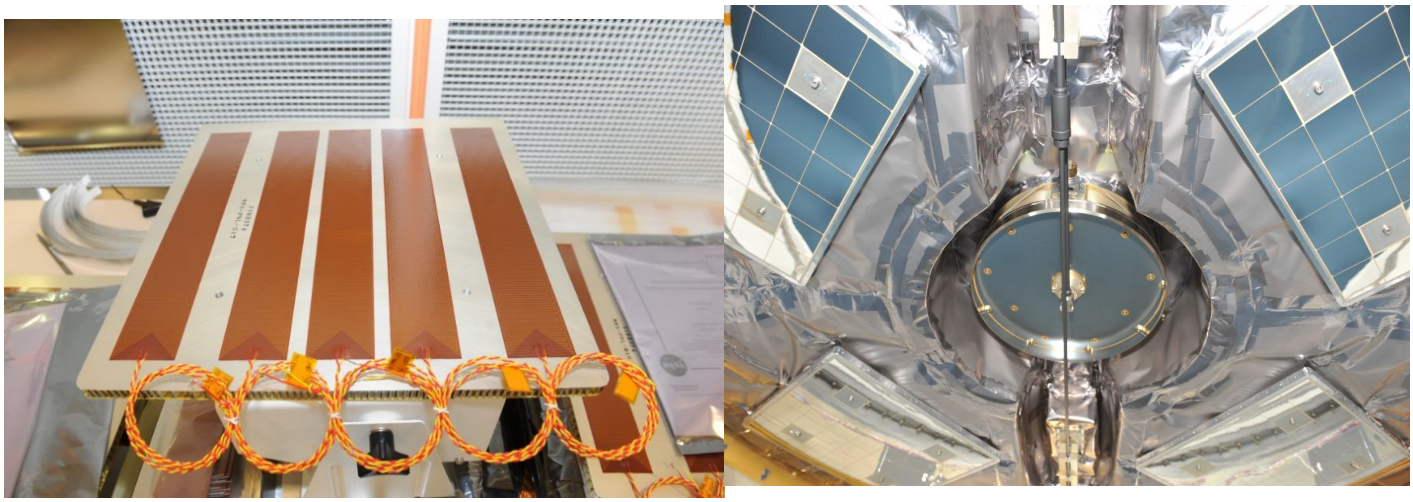

Figure 9. Shunt resistor (*left*); four radiators with OSR covers (*right*).

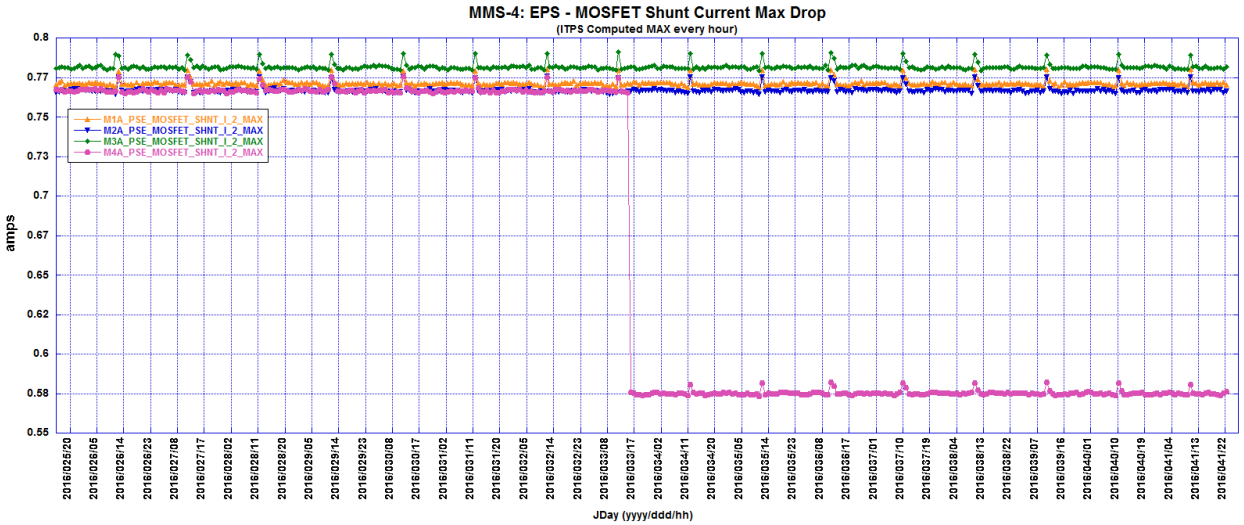

Figure 10. Reduced shunt radiator current.

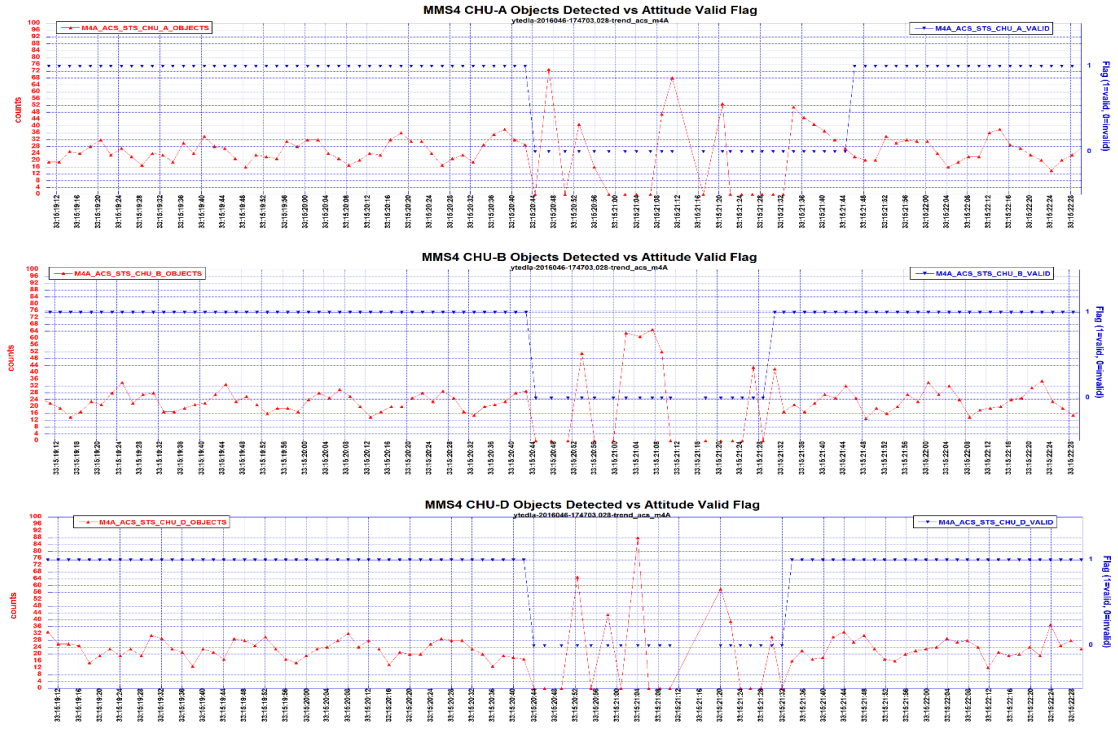

Figure 11. Star camera non-star objects (*red*) and range of valid solutions (*blue*).

Another very suggestive piece of on-board data was that the FIELDS science instruments detected a sudden plasma event on each of its six detectors (Fig. 12), with this most pronounced, and persisting for longest, in the –Z spacecraft direction. From the size of the voltage change that was observed, it can be deduced that the impactor was larger than that for a "typical" spacecraft micrometeoroid hit. Finally, a piece of negative data was that there was no sign in power system telemetry that a malfunction such as a venting battery cell had occurred. (Such events have been observed on other spacecraft in the past, such as Mariner 7 just prior to its encounter with Mars in 1969.)

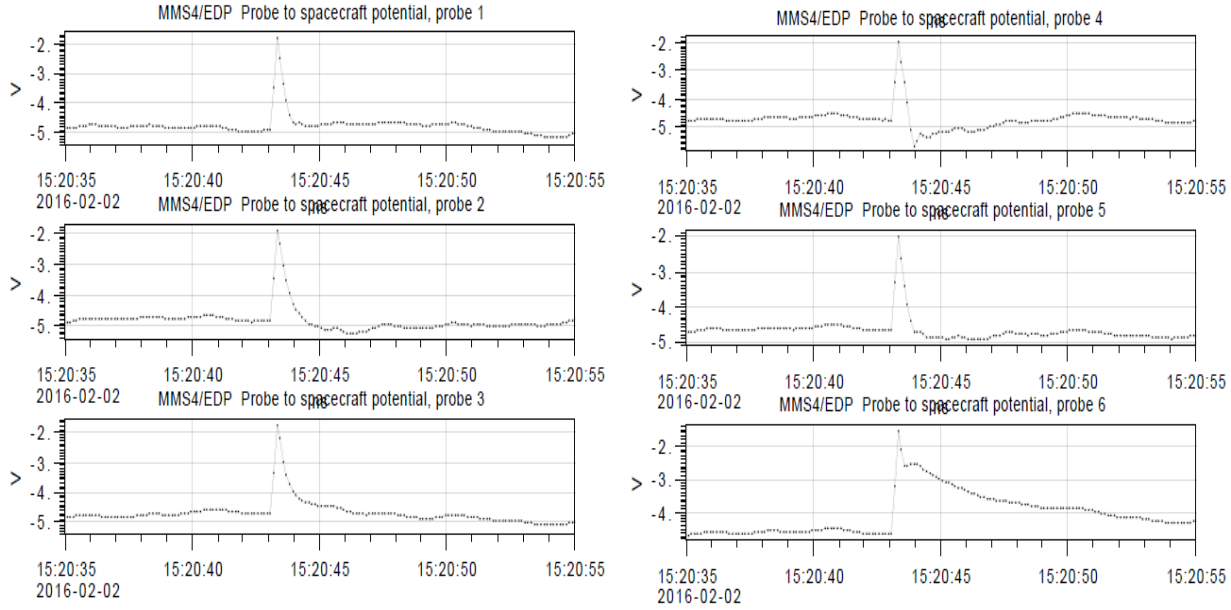

Figure 12. FIELDS plasma data (Probe 6 on –Z ADP boom).

It therefore appeared clear that MMS had suffered a micrometeoroid/orbital debris (MMOD) hit, with this impacting the radiator, throwing out material including plasma and highly reflective shards of OSR, and traveling through to sever one of the shunt resistors. A key question was to try to determine how massive the impacting body was, and therefore estimate the kinetic energy that may have been involved in the collision.

B. Analysis Method

A check was first carried out to see if the impact event could be observed in the data from the MMS GPS-Enhanced Onboard Navigation System (GEONS) navigation system: however, this did not reveal any signature. Since GEONS is very sensitive, the delta-v that was imparted to the spacecraft by the impact must therefore have been modest. In order to analyze the impact, the initial accelerometer transients along the three body axes (see Fig. 13) were then examined so as to be able to estimate the direction of impact. (The later accelerometer data was not used, as it was expected to be heavily affected by structural vibrations, etc. In addition, the accelerometer data is only sampled every 30 s, making its utility for detailed calculations doubtful.) The initial spikes were found to be -0.8 μg along the X-axis, 2.8 μg along Y and -1.7 μg along Z, giving an estimated impact direction 30.3 deg below the MMS spin plane.

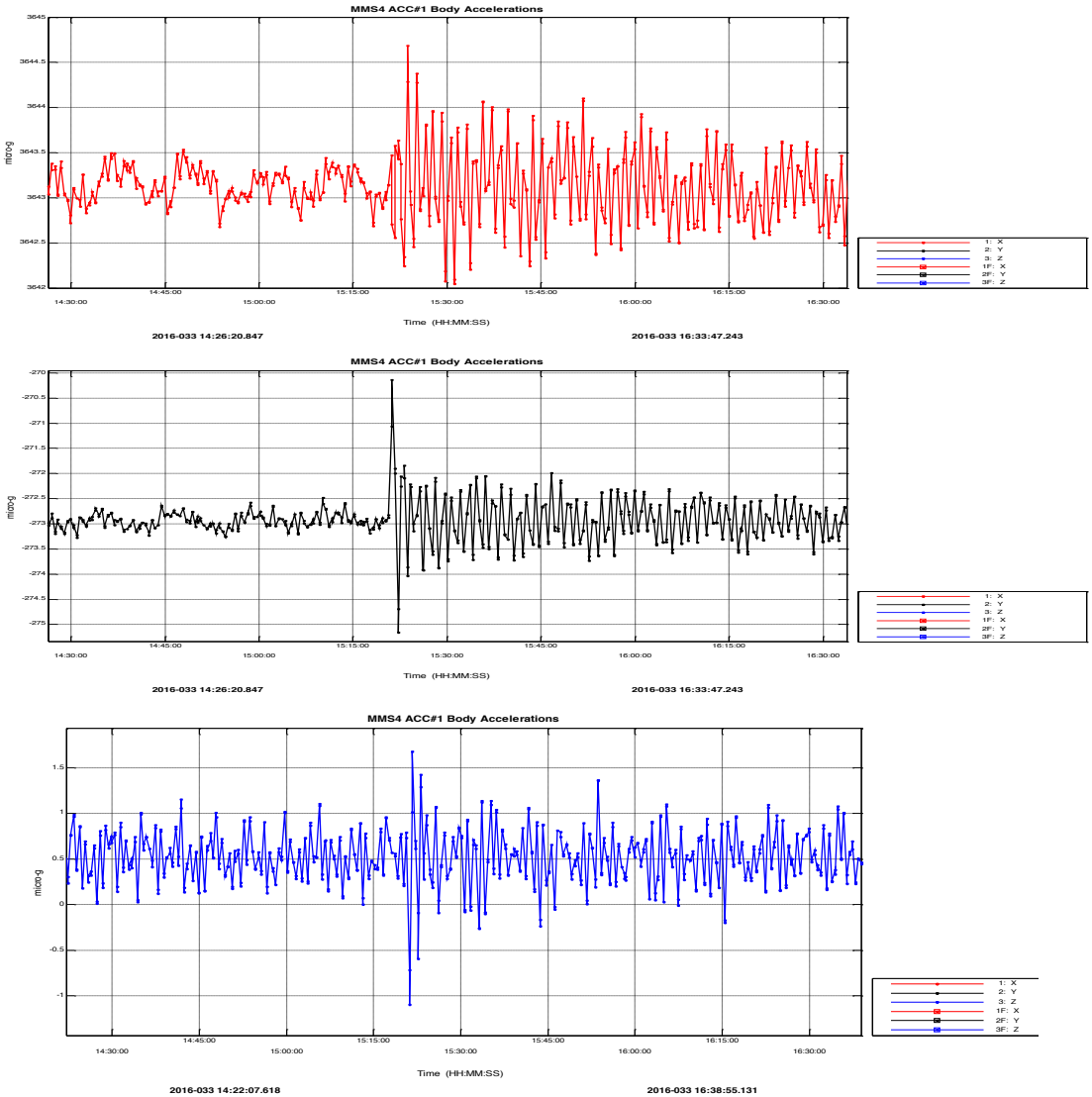

Figure 13. Accelerometer data at time of impact.

Fig. 14 shows the transverse rotation rates at the time of the impact: the increases in nutation and boom vibration caused by the event are evident, as is the brief data dropout caused by the blinding of the star cameras. By contrast, Fig. 15 shows that no change in axial spin rate was produced. This makes sense given the fact that the location of the impact was near the centerline of the spacecraft.

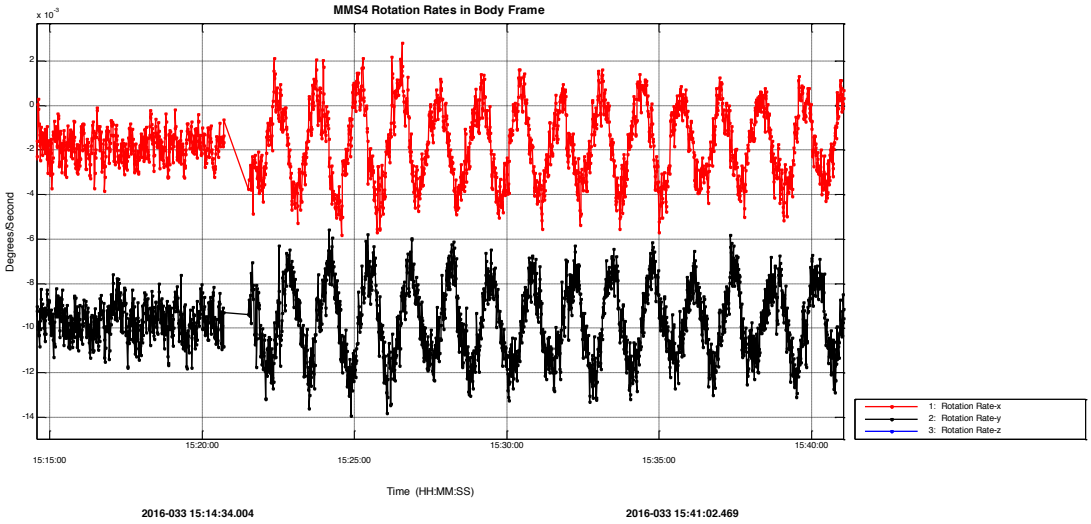

Figure 14. Transverse rotation rates at time of impact.

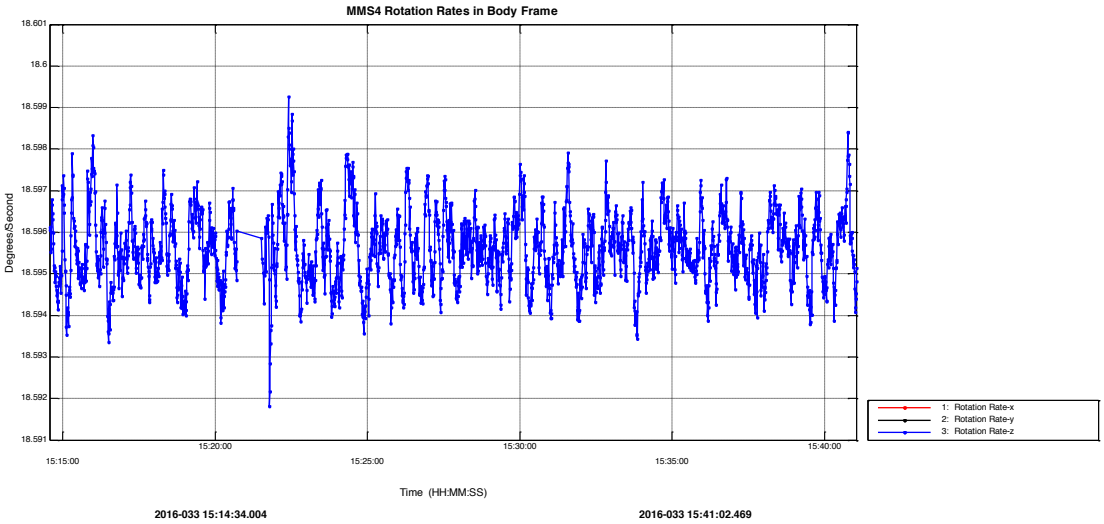

Figure 15. Axial rotation rate at time of impact.

A key measurement that was used in this analysis was the angle between the major principal axis (loosely, the spin axis) and the Ecliptic North Pole. (This quantity will be referred to here, for brevity, as the spacecraft pointing angle.) This mean value of this angle was found to change by 0.00157 deg as a result of the impact: this shift is small, but not so small as to be an unreliable quantity. It can therefore be used as the basis for calculations to quantify the impact.

One initial question is whether the observed dynamics are consistent with the assumption that the spacecraft was struck by an impactor of some sort. To examine this, Fig. 16 gives a time history of the pointing angle for a period soon after the impact; Fig. 17 is the corresponding Fast Fourier Transform (FFT) frequency response. It can be seen from both of these plots that a large component of the response is made up of a low-frequency component, with a period of approximately 400 s (i.e. a frequency of 0.15 RPM). This appears highly likely to be a vibration mode of the 60 meter long MMS wire booms. In order to verify this, the pointing angle after a recent spacecraft Delta-V maneuver was examined (see Fig. 18): this exhibits an oscillation with the same period of about 400 s. This motion is known to represent wire boom dynamics that are excited by the acceleration of the central spacecraft body by the

thrusters. The observed response in Figs. 16 and 17 is therefore consistent with acceleration of the central spacecraft caused by an impact.

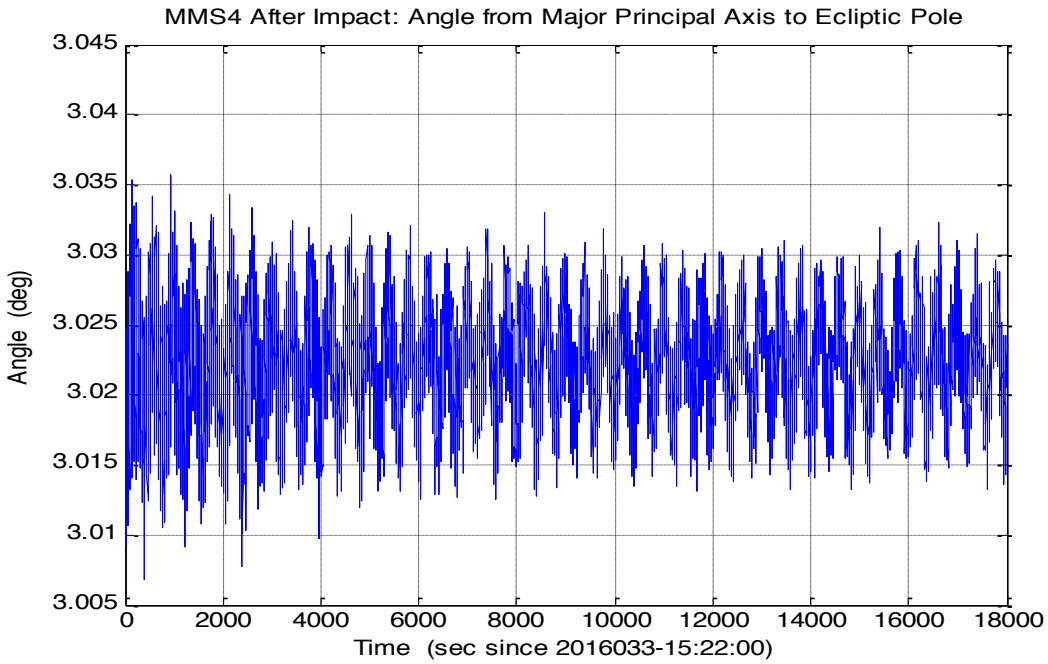

Figure 16. Pointing angle after event.

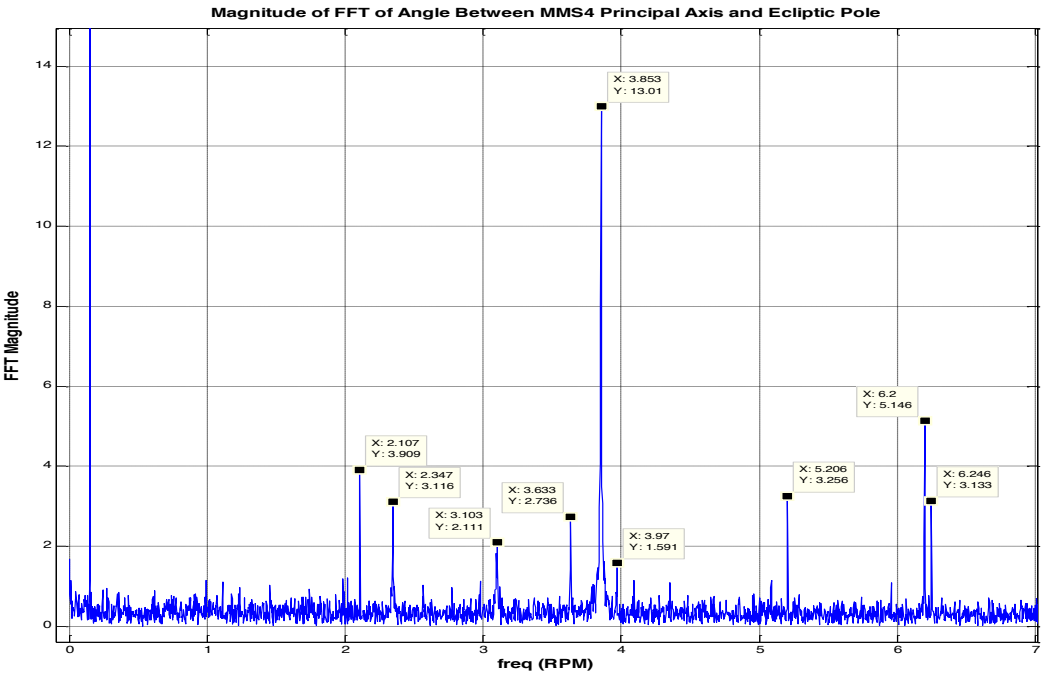

Figure 17. Fast Fourier Transform of pointing angle after event.

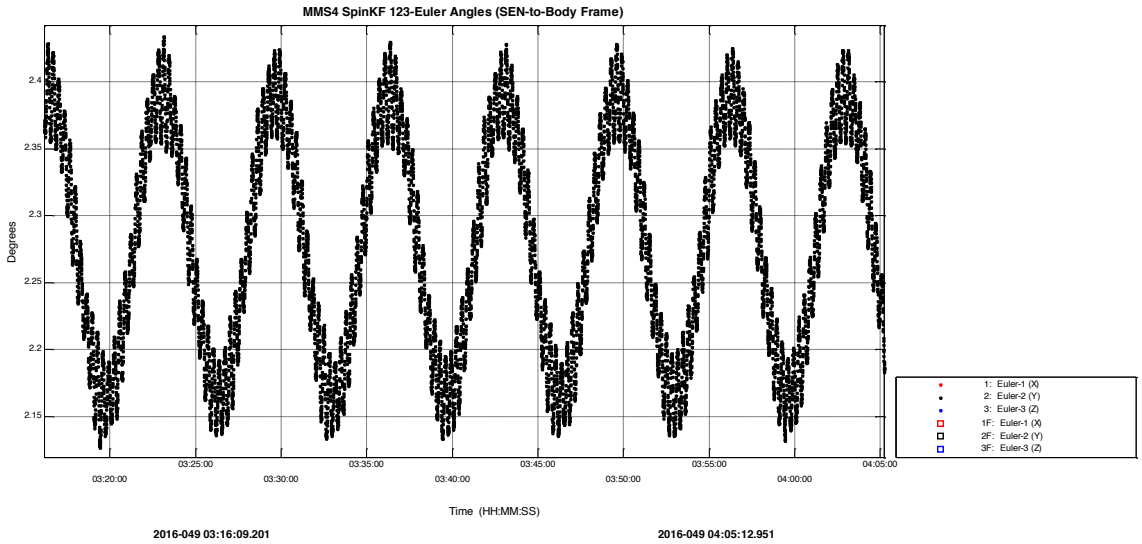

Figure 18. Pointing angle after recent typical maneuver.

In order to analyze the MMS4 impact event, the following analysis sequence was used:

- Use the change in MMS pointing angle produced by the impact, together with the known spacecraft angular momentum, to derive the transverse angular momentum that is applied to the spacecraft by the impactor
- From the known impact point on the spacecraft and the estimated impact direction, this allows the linear momentum of the impactor relative to MMS to be computed
- From the known position of MMS on its orbit at the time of impact, its orbital velocity at that point can be found
- For an assumed impactor population, its speed relative to MMS can then be estimated
- Given the linear momentum and speed of the impactor, its mass can be derived
- This mass and the relative speed can finally be used to estimate the kinetic energy of the impact.

C. Results

The method outlined above was applied to two assumed possible impactor populations: micrometeoroids, and orbital debris originating in geosynchronous orbit (GEO). The impact point was at a radius of 48,176 km (7.553 R_E): this is 6,012 km above the GEO ring. In addition, it was at latitude -21.2 deg, and so 17,403 km below the GEO equatorial plane. It may therefore not at first seem possible that the impactor could have originated in the GEO ring. However, it has been shown [10][11] that the action of solar radiation pressure (SRP) on objects with high area/mass ratios (greater than around 15 m^2/kg) can lead to significant perturbations to both eccentricity (and hence radius) and inclination. In particular, it is possible for a high area/mass object to originate in GEO and reach the MMS4 impact point. A particular candidate object that will be considered here is a small fragment of multi-layer insulation (MLI) from a GEO satellite: a typical layer of MLI has an area/mass ratio of around 25 m^2/kg, and so is in the high A/m range considered in [10][11]. MLI is known to degrade and become brittle under GEO conditions, so it appears possible for a fragment to become liberated, then have its orbit be perturbed by SRP until it reaches the impact point.

Applying the analysis sequence that was previously described, the change of spacecraft pointing angle, together with the known angular momentum of the spacecraft and the known impact point location and approach angle, imply that the linear momentum that was applied to the spacecraft by the impact was approximately 0.127 kg m/s, regardless of the impactor population that is assumed. Note that this corresponds to a delta-v applied to MMS4 of less than 0.1 mm/s: this is small enough that it makes sense that it was not observed by the GEONS navigation system.

The two impactor candidate populations will now be considered in turn. Note that it does not appear possible, based on the data available for this analysis, to decide which of these two types was what actually struck MMS4.

In the case of a micrometeoroid, a "typical" approach speed of 15 km/s will be assumed. This then implies that the mass of the particle was around 8.48×10^{-3} gm: this is at the large end of the micrometeoroid size spectrum, which reaches its peak in the range 10^{-8} to 10^{-3} gm, but it appears possible. This mass corresponds to a particle with a diameter of around 2 mm. The resulting estimated kinetic energy of the impact with MMS4 is 954 J: to put this into context, it is roughly equivalent to 47% of the muzzle energy of an AK-47 rifle.

Consider now the case of an MLI fragment originating in GEO. The orbital velocity of MMS4 at the time of the impact was 2.661 km/s. If the impactor is on an orbit that started as GEO and was then perturbed to have increased eccentricity and inclination (so to reach the impact point), the relative speed between impactor and spacecraft at impact will then be around 4.292 km/s, with the precise value depending on the exact geometry of the approach trajectory. This is considerably lower than for the micrometeoroid case, so requiring a higher impactor mass in order to reach the specified linear momentum value. Specifically, the mass in this case is found to be 2.96×10^{-2} gm: if this consists of a fragment of MLI with area/mass ratio 25 m^2/kg, it corresponds to a square 2.72 cm on a side. The resulting impact kinetic energy in this case is only 273 J, or 13% of the muzzle energy of an AK-47. This difference in kinetic energy may possibly provide a clue as to which of the two candidate impactor populations actually hit MMS4, if it can be correlated to the damage that was done to the spacecraft in the impact. However, this is beyond the scope of the current paper.

V. Conclusions

This paper has used the extensive attitude dynamics data that is collected by MMS to quantify the observed effects of the various environmental disturbance torques that act on the spacecraft. In addition, the slow decay in spin rate that has been observed to occur for all four spacecraft was analyzed, and shown to be consistent with the effects of the disturbance torque produced by the ASPOC devices. Finally, attitude dynamics data was shown to be key to analyzing the MMS4 micrometeoroid/orbital debris impact event that occurred on Feb. 2, 2016.

Acknowledgements

The authors wish to acknowledge the invaluable contributions of the other members of the MMS Flight Dynamics team, especially Maryam Bakhtiari-Nejad, Babak Vint and Mark Godine.

References

[1] A.S. Sharma and S.A. Curtis, "Magnetospheric Multiscale Mission", *Nonequilibrium Phenomena in Plasmas*, Astrophysics and Space Science Library Vol. 321, Springer-Netherlands. pp. 179–195, 2005.

[2] T. Williams, "Launch Window Analysis for the Magnetospheric Multiscale Mission", Paper AAS12-255, AAS/AIAA Space Flight Mechanics Meeting, Charleston, SC, Jan./Feb. 2013.

[3] D.H. Fairfield, "A Statistical Determination of the Shape and Position of the Geomagnetic Neutral Sheet", *J. Geophysical Research*, Vol. 85, No. A2, pp. 775-780, Feb. 1980.

[4] D.J. Chai, S.Z. Queen and S.J. Placanica, "Precision Closed-Loop Orbital Maneuvering System Design and Performance for the Magnetospheric Multiscale Formation", Paper 181, 25th International Symposium on Space Flight Dynamics, Munich, Germany, Oct. 2015.

[5] J.C. Raymond, J.E. Sedlak and B. Vint, "Attitude Ground System (AGS) for the Magnetospheric Multiscale (MMS) Mission", 25th International Symposium on Space Flight Dynamics, Munich, Germany, Oct. 2015.

[6] J.R. Wertz, (ed.), *Spacecraft Attitude Determination and Control*, D. Reidel Publishing Company, Dordrecht, The Netherlands, 1978.

[7] T. Williams, N. Ottenstein, E. Palmer and M. Farahmand, "Initial Satellite Formation Flight Results from the Magnetospheric Multiscale Mission", AIAA SPACE-2016 Conference, Los Angeles, CA, Sept. 2016.

[8] A. Genovese, M. Tajmar, N. Buldrini and W. Steiger. "2000-Hour Endurance Test of Indium Field Emission Electric Propulsion Microthruster Cluster." *Journal of Propulsion and Power*, Vol. 20, No. 2, pp. 219-27, 2004.

[9] M. Tajmar, A. Genovese and W. Steiger. "Indium FEEP Microthruster Experimental Characterization." Web. 10 May 2016.

[10] A.J. Rosengren and D.J. Scheeres, "Long-term dynamics of high area-to-mass ratio objects in high-Earth orbit", *Advances in Space Research*, Vol. 52, No. 8, p. 1545-1560, 2013.

[11] C. Pardini and L. Anselmo, "Long-Term Evolution of Geosynchronous Orbital Debris with High Area-to-Mass Ratios", *Trans. Japan Soc. Aero. Space Sci.*, Vol. 51, p. 171, Apr. 2007.